Methods and systems of polarization reproduction and analysis of the biological layers structure in the diagnosis of pathologies

Zabolotna, Natalia, Sholota, Vladyslava, Okarskyi, Heorhii

Natalia I. Zabolotna, Vladyslava V. Sholota, Heorhii H. Okarskyi, "Methods and systems of polarization reproduction and analysis of the biological layers structure in the diagnosis of pathologies," Proc. SPIE 11369, Fourteenth International Conference on Correlation Optics, 113691S (6 February 2020); doi: 10.1117/12.2556542

SPIE.

Event: Fourteenth International Conference on Correlation Optics, 2019, Chernivtsi, Ukraine

Methods and systems of polarization reproduction and analysis of the biological layers structure in the diagnosis of pathologies

Natalia I. Zabolotna[a], Vladyslava V. Sholota[a], Heorhii H. Okarskyi[a]
[a]Vinnytsia National Technical University, 95 Khmelnytske Shose, Vinnytsia, Ukraine

ABSTRACT

Methods and automated systems of direct and Mueller-matrix reproduction of optical anisotropy parameters (orientation of the fast axis and optical phase shift) of two-layer optically thin biological structures are represented. The pathological condition objective assessment is based on the multi-parameter analysis of statistical characteristics (estimates of starting moments of the first order and estimates of the central moments of the second to fourth orders) determined for the coordinate, autocorrelation distributions and logarithmic dependences of the power spectra of the distributions of reproducible anisotropy parameters biological layers. The accuracy of the suggested methods of polarized phase reproduction and analysis of the biological layers structure within the range of 83.7% to 95.3% is estimated.

Keywords: biological layer, two-layer biological tissue, optical anisotropy, polarization-phase reproduction, Mueller matrix, statistical analysis, autocorrelation analysis, power distribution spectrum**.**

1. INTRODUCTION

One of the pressing problems of modern medical instrumentation is the development of advanced new methods and means of effective diagnostics and objective monitoring of the human body condition with the improvement of reliability of the assessment of pathological conditions.

Irradiation of histological sections of biological tissues (BT) and films of biological fluids (BF) by polarized light of the visible and near infrared spectra is a promising approach to the development of modern opto-electronic technologies of medical diagnostics[1-19]. This allows us to obtain qualitatively new results in studies of the morphological and functional states of biological layers due to the high sensitivity of the polarization characteristics of scattered fields to the optical properties and geometry of biological environment.

Recent years, a new field of diagnostics of biological tissues and liquids, based on polarization methods and means of reproduction of structural anisotropy of biological layers in the form of two-dimensional images and the application of modern computer technologies of image analysis has formed[13,19].

In order to determine the objective parameters characterizing the changes of optical anisotropy (axis orientation and optical phase shift proportional to birefringence) of biological layers, statistical, correlation and fractal analysis of polarization and Mueller distributions of the values of polarization and Mueller parameters were applied in this direction[20-22]. Based on that, pathological changes in the optically thin biological layers of the dermis, epithelial or other tissues caused by malignant conditions and inflammatory processes of human organs, particularly during the early stages of development, are differentiated and evaluated. Such successful diagnostic application of laser polarimetry methods and tools in the diagnosis of the structure of optically thin biological layers objectively stimulates their further development and spread to more complex multilayer biological structures (BS).

It should be noted that in our time there is no single approach to the creation of methods and means of polarization-phase reproduction of the structure of multilayered biological tissues and multivariable objective analysis of the obtained data. This causes the lack of reliability of the evaluation of pathological conditions of real biological structures under conditions of multiple scattering of irradiating polarizing beam. On the other hand, under the conditions of single scattering, the main drawback of the existing methods and means of polarization and Mueller-matrix mapping of biological layers is the lack of reproducibility of the experimental data, which also limits the validity of diagnosing pathological conditions.

The purpose of this work is to investigate the possibility of improving the reliability of pathology evaluation in systems of polarization diagnosis of histological sections of biological tissues by applying new methods and systems of polarization-phase reproduction and analysis of the structure of biological layers and two-layer polycrystalline biological networks.

Fourteenth International Conference on Correlation Optics, edited by
Oleg V. Angelsky, Proc. of SPIE Vol. 11369, 113691S · © 2020 SPIE
CCC code: 0277-786X/20/$21 · doi: 10.1117/12.2556542

2. BASIC DEFINITIONS AND ANALYTICAL RELATIONS

It`s known that the basic equation for the transformation of polarization radiation, which is transmitted through the optically thin sample (extinction coefficient $\tau \le 0,01$) of biological layer (BL) at point $(x,y)\left(x=\overline{1;M};y=\overline{1;N}\right)$, connects Stokes vectors $\mathbf{S}_*^{(x,y)},\mathbf{S}_0^{(x,y)}$ converted and input polarized radiation, in accordance to a Mueller matrix of the biological layer $\mathbf{Z}^{(x,y)}$.

$$\mathbf{S}_*^{(x,y)}=\mathbf{Z}^{(x,y)}\times\mathbf{S}_0^{(x,y)}, \tag{1}$$

where $M\times N$ is the set of image pixels of a sample of a biological layer.

The Mueller matrix $\mathbf{Z}^{(x,y)}$ that reproduces the optically anisotropic properties of an optically thin biological layer according to the polycrystalline model of its representation at each point (x,y) is determined by the formula

$$\mathbf{Z}^{(x,y)}=\begin{Vmatrix}1 & 0 & 0 & 0\\ 0 & z_{22}^{(x,y)} & z_{23}^{(x,y)} & z_{24}^{(x,y)}\\ 0 & z_{32}^{(x,y)} & z_{33}^{(x,y)} & z_{34}^{(x,y)}\\ 0 & z_{42}^{(x,y)} & z_{43}^{(x,y)} & z_{44}^{(x,y)}\end{Vmatrix},\ z_{ik}^{(x,y)}=\begin{cases}z_{22}^{(x,y)}=\cos^2 2\rho^{(x,y)}+\sin^2 2\rho^{(x,y)}\cos\delta^{(x,y)};\\ z_{23;32}^{(x,y)}=\cos 2\rho^{(x,y)}\sin 2\rho^{(x,y)}\left(1-\cos\delta^{(x,y)}\right);\\ z_{33}^{(x,y)}=\sin^2 2\rho^{(x,y)}+\cos^2 2\rho^{(x,y)}\cos\delta^{(x,y)};\\ z_{34;43}^{(x,y)}=\pm\cos 2\rho^{(x,y)}\sin\delta^{(x,y)};\\ z_{24;42}^{(x,y)}=\pm\sin 2\rho^{(x,y)}\sin\delta^{(x,y)};\\ z_{44}^{(x,y)}=\cos\delta^{(x,y)},\end{cases} \tag{2}$$

where $\rho^{(x,y)}$ -

$$\mathbf{Z}^{(x,y)}=\mathbf{B}^{(x,y)}\times\mathbf{A}^{(x,y)}. \tag{3}$$

Therefore, MMI elements of two-layer BL is described by complex superposition of orientations $(\rho_A^{(x,y)};\rho_B^{(x,y)})$ and phase $(\delta_A^{(x,y)};\delta_B^{(x,y)})$ parameters biological layers $\mathbf{A}^{(x,y)}$ and $\mathbf{B}^{(x,y)}$ that is illustrated by the example element

$$z_{44}^{(x,y)}=\cos(2\rho_A^{(x,y)}-2\rho_B^{(x,y)})\sin\delta_A^{(x,y)}\sin\delta_B^{(x,y)}+\cos\delta_A^{(x,y)}\cos\delta_B^{(x,y)}. \tag{4}$$

However, exact reproduction of the orientation-phase structure of the internal layer $\mathbf{B}^{(x,y)}=\left\{b_{ik}^{(x,y)}(\rho_B,\delta_B)\right\}$ on the background of the external layer $\mathbf{A}^{(x,y)}=\left\{a_{ik}^{(x,y)}(\rho_A,\delta_B)\right\}$ based on the well-known MMI two-layer BL is mathematically incorrect and physically controversial.

Considering above, the simplified approach to solving the problem of reproduction of orientation and phase parameters of anisotropy of two-layer biological tissues is applied based on estimation of statistical, correlation and fractal characteristics of transformation of polarization-phase parameters of radiation by two-layer biological structures[20-22].

Statistical analysis of coordinate distribution $\mathbf{Z}_{ik}(M,N)$ of MMI elements is implemented by determining the estimate of the starting moment of the first order (M_1) and from the second to the fourth central moment estimates $\left(M_2-M_4\right)$, by following expressions[20-22]

$$M_1 = \frac{1}{MN}\sum_{j=1}^{MN}\left(z_{lk}\right)_j; \qquad M_2 = \sqrt{\frac{1}{MN}\sum_{j=1}^{MN}\left(\left(\overset{\circ}{z}_{lk}\right)_j\right)^2};$$
$$M_3 = \frac{1}{M_2^3}\frac{1}{MN}\sum_{j=1}^{MN}\left(\left(\overset{\circ}{z}_{lk}\right)_j\right)^3; \qquad M_4 = \frac{1}{M_2^4}\frac{1}{MN}\sum_{j=1}^{MN}\left(\left(\overset{\circ}{z}_{lk}\right)_j\right)^4, \tag{5}$$

where $M \times N -$ quantity of pixels of the camera's photosensitive matrix; $(\overset{\circ}{z}_{lk}) -$ centered element z_{lk}.

Statistical characteristics of distributions of autocorrelation functions (ACF) $\overline{K}(s)$ of MMI elements $\mathbf{Z}_{ik}(M,N)$ are determined in the form of estimates of the starting moment of the first order (Q_1) and from the second to the fourth orders central moment estimates $\left(Q_2 - Q_4\right)$

$$Q_1 = \frac{1}{2M}\sum_{s=0}^{2M-1}\overline{\mathbf{K}(s)}; \qquad Q_2 = \sqrt{\frac{1}{2M-1}\sum_{s=0}^{2M-1}\left(\overline{\mathbf{K}}(s) - Q_1\right)^2}$$
$$Q_3 = \frac{1}{Q_2^3}\frac{1}{2M-1}\sum_{s=0}^{2M-1}\left(\overline{\mathbf{K}}(s) - Q_1\right)^3; \qquad Q_4 = \frac{1}{Q_2^4}\frac{1}{2M-1}\sum_{s=0}^{2M-1}\left(\overline{\mathbf{K}}(s) - Q_1\right)^4. \tag{6}$$

Statistical evaluation of power distribution spectra $\mathbf{Z}_{ik}(X,Y)$ represented in logarithmic axes $\log(PSD_{ik}(\nu)) - \log(\nu)$ assumes the determination of the starting moment estimate of the first order $\left(W_1\right)$ and from the second to the fourth orders of central moments estimates $\left(W_2 - W_4\right)$ of distribution of logarithmic dependences $\log\left(PSD_{Z_{lk}}(\nu)\right) - \log(\nu)$ of MMI power spectra

$$W_1 = \frac{1}{N}\sum_{d=1}^{N}\left(\log PSD\ (\nu)\right);$$
$$W_2 = \sqrt{\frac{1}{N}\sum_{d=1}^{N}\left(\log PSD(\nu) - W_1\right)^2};$$
$$W_3 = \frac{1}{W_2^3}\frac{1}{N}\sum_{d=1}^{N}\left(\log PSD(\nu) - W_1\right)^3; \tag{7}$$
$$W_4 = \frac{1}{W_2^4}\frac{1}{N}\sum_{d=1}^{N}\left(\log PSD(\nu) - W_1\right)^4.$$

($\nu = \frac{1}{d}$ - frequency of appearance in two-dimensional distribution of structural elements with dimensions $\left(d = 2\mu m \div 2000\mu m\right)$).

3. METHODS AND SYSTEMS OF POLARIZATION REPRODUCTION AND ANALYSIS OF BIOLOGICAL LAYERS

High sensitivity of a set of statistical characteristics of coordinate distributions, AKF and power spectra is determined by the distributions of elements of orientation and phase maps of biological layers reproduced from the corresponding MMI to changes in the parameters of their phase structural anisotropy due to pathological conditions.

The next step of the research is to develop methods of direct (without calculation of MMI) polarization-phase reproduction of the orientation-phase structure of an optically thin BL.

To implement method of direct polarization reproduction and analysis of the distribution of orientation parameters of an optically thin biological sample by the corresponding system illustrated in figure 1 one should:

1. To make the polarization-angular scanning of the biological sample in the range $0 \le \theta_i \le 180$ with a step of $\Delta\theta$ by series of linearly polarized laser beams with azimuth polarization $\alpha = \theta_i + \Delta\theta$ at a wavelength of 0.632 μm.
2. To filter the obtained distributions of linearly polarized laser beams transmitted through the biological sample by means of crossed " polarizer-analyzer " synchronously rotating at an angle α at each step.
3. To record and analyze in the plane of the digital camera a series of polarized filtered images $I_\alpha(x, y)$. If in any point $I(x, y) = 0$, then orientation optical axis is $\rho(x, y)$ of polycrystalline sample network $\rho(x, y) = \alpha$.
4. To obtain a series of coordinate distributions of the orientational parameters of a polycrystalline structure of a biological sample $\rho(X, Y) \equiv R(\theta_i), X = \overline{1:M}, Y = \overline{1:N}$.
5. To determine statistical estimates of coordinate distribution, autocorrelation function and logarithmic dependences of power spectra of distributions of orientation parameters of biological sample, which are informative parameters for further diagnosis.

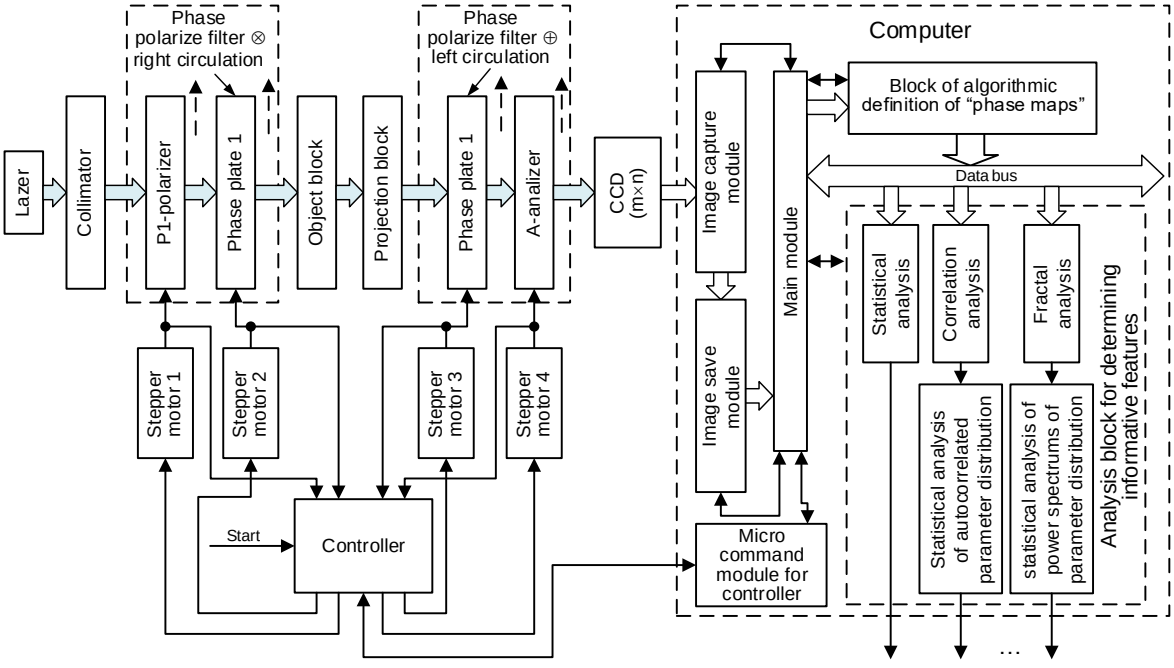

Figure 1. System of direct polarization reproduction and analysis of the distribution of orientation parameters of an optically thin biological sample

To implement method of direct polarization reproduction and analysis of the distribution of phase parameters of an optically thin biological sample by the corresponding system illustrated in figure 2 one should:

1. To irradiate the biological sample with a laser polarization beam "right circulation" at a wavelength of 0.632 μm .
2. To project the formed image in the plane of the digital camera.
3. To realize polarization filtering of the sample image by means of the polarization filter "left circulation".
4. To record a filtered image in the plane of the camera. According to the coordinate distribution of image intensities, obtain the phase shift distribution $\delta(x, y) = 2\arcsin\sqrt{I(x, y)}$.
5. To determine statistical estimates of coordinate distribution, autocorrelation function and logarithmic dependences of power spectra of distributions of phase parameters $\delta(X, Y)$ of biological sample, which are informative parameters for further diagnosis.

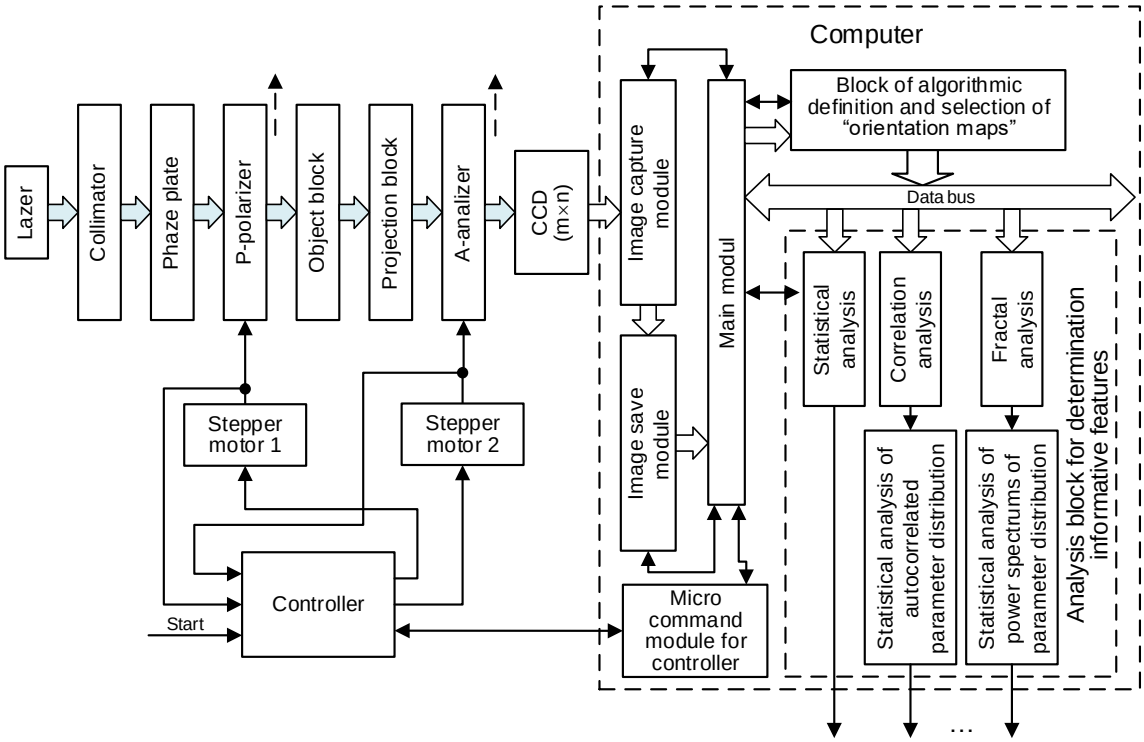

Figure 2. System of direct polarization reproduction and analysis of the distribution of phase parameters of an optically thin biological sample

Generalization on the multilayer biological tissues of the idea of polarization state variation of the laser beam irradiating BL and the change monitoring in the parameters of the Stokes vector $\mathbf{S}_{i=1\div4}$ at points (x, y) of its polarization-inhomogeneous image formed the basis of the Mueller-matrix reproduction of the coordinate distributions of the orientation and phase parameters of the structure "screened" outside of the two-layer optically thin BL.

To implement the method of Mueller-matrix reproduction of coordinate distributions of orientation and phase parameters of "screened" outside layers structure of optically thin two-layer biological tissue by the corresponding system illustrated in figure 3 one should:

1. To rotate the angle $\theta_i = \theta_{i-1} + \theta$ of plane of polarization of the laser beam $(\alpha_0, \beta_0)(\alpha_0 = \theta_0)$ at each current i-th measurement step using a polarizing linear filter which irradiates the biological sample at a wavelength of 0.632 μm.

2. To create six coordinate distributions of polarized filtered radiation intensities recorded by a digital camera at each i-th step, irradiation using a polarization analyzer and a phase plate. On this basis, algorithmically determine the distributions of a set of Stokes vector parameters $\mathbf{S}_{1;2;3;4}^{(\theta_i)}(X,Y)$.

3. To determinate coordinates of pixels (m,n) photosensitive camera matrix $(m=\overline{1;M};n=\overline{1;N})$ based on the analysis of the condition $(S_2^{(\theta)}(m,n))^2+(S_3^{(\theta)}(m,n))^2+(S_4^{(\theta)}(m,n))^2\to 1$ between coordinate distributions of Stokes vector parameters for which the optimal polarization state of the irradiating beam is formed at a given current angle θ of rotation of its polarization plane.

4. To determinate the corresponding values of the directions of orientation of the optical axes $\rho_A(m,n);\rho_B(m,n)$ and phase shifts $\delta_A(m,n);\delta_B(m,n)$ of the internal and external layer of the two-layer biological tissue for found coordinates (m,n) photosensitive camera matrix $(m=\overline{1;M};n=\overline{1;N})$ ratio-based algorithmically

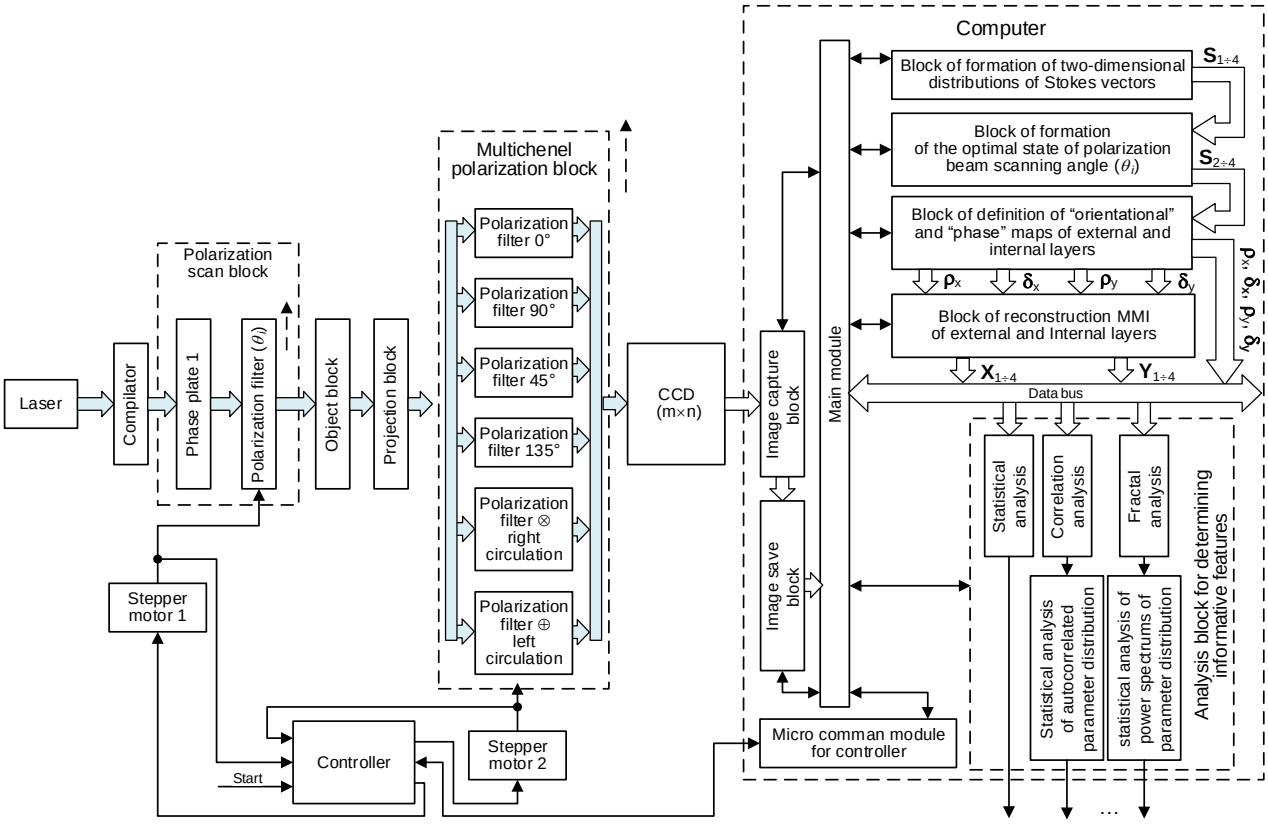

Figure 3. System of Mueller-matrix reproduction of coordinate distributions of orientation and phase parameters of structure of "screened" outside layers of optically thin two-layer biological tissue

$$\begin{cases}\delta_A^{(x,y)}=\arccos\left(\pm\sqrt{1+\dfrac{1-\cos\left(\delta_B^{(x,y)}\right)}{\cos^2\left(2\left(\rho_A^{(x,y)}-\rho_B^{(x,y)}\right)\left(1+\delta_A^{(x,y)}\right)\right)}}\right);\\ \delta_B^{(x,y)}=\arccos\left[S_4^{(x,y)}(\theta)\right].\end{cases} \tag{8}$$

$$\begin{cases} \rho_A^{(x,y)} = 0,25\pi + \theta; \\ \rho_B^{(x,y)} = 0,5 arctg\left(S_3^{(x,y)}(\theta) \Big/ S_2^{(x,y)}(\theta) \right). \end{cases} \quad (9)$$

5. To repeat claims 1-4 for all measurement steps θ_i within the complete rotation of the polarization plane $\left(0 \le \theta_i \le \pi\right)$, thereby determining the coordinate distributions of the reproduced orientation $\mathbf{\rho}_A(X,Y); \mathbf{\rho}_B(X,Y)$ and phase parameters $\mathbf{\delta}_A(X,Y); \mathbf{\delta}_B(X,Y)$ of the biological layers of the two-layer biological tissue.

6. To determinate statistical estimates of the coordinate distribution, autocorrelation function and logarithmic dependences of the power spectra of the distributions of the reproduced orientation and phase parameters of the subsurface layers of a two-layer biological structure to determine the informative parameters of further differentiation of their states due to pathological changes.

4. IMPLEMENTATION AND TESTING OF MULTI-PARAMETER SYSTEM OF REPRODUCTION AND ANALYSIS OF THE STRUCTURE OF BIOLOGICAL LAYERS

The multiparameter system of polarization-phase reproduction and analysis of the anisotropy parameters of planar biological tissues and liquids shown in figure. 4 allows to measure the polarization parameters of images of biological layers, reproduce the anisotropy parameters of the structure of single-layer and two-layer biological objects based on the methods mentioned above, implement their intellectual analysis to determine the totality of informative features while supporting decision-making in the process of diagnosing biological layers.

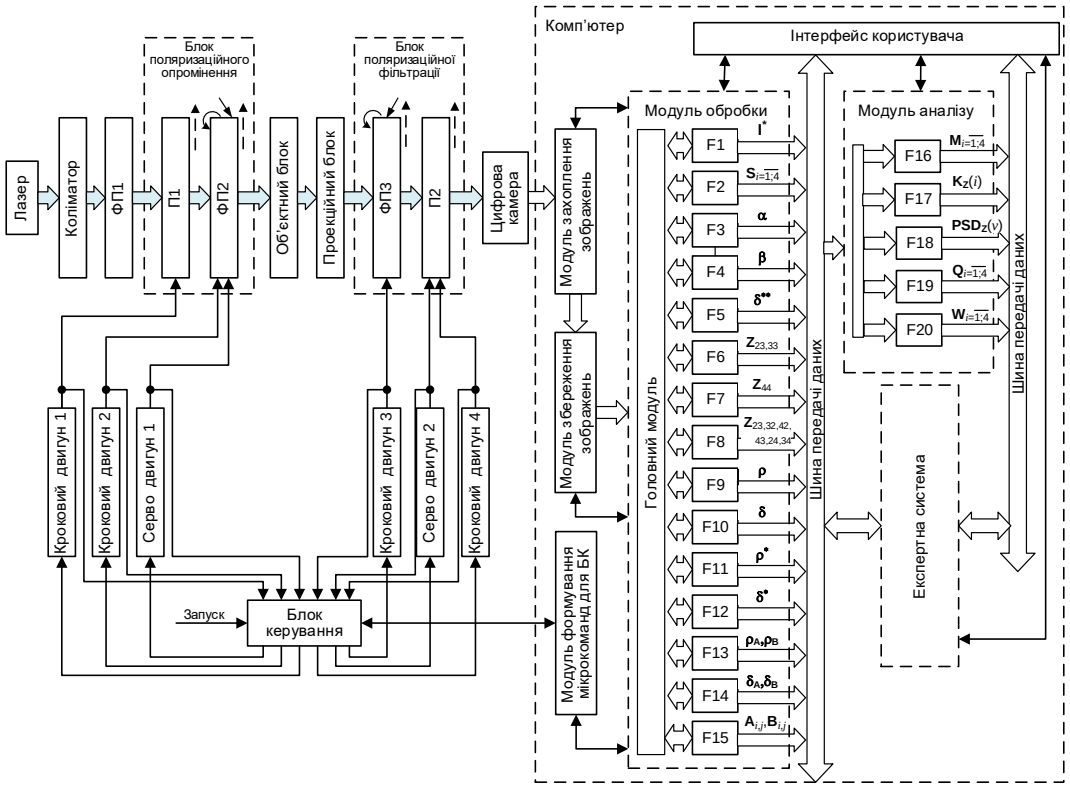

Figure 4. Architecture of a multi-parameter imaging system polarization-phase reproduction and analysis of anisotropy parameters of planar biological tissues and liquids

The system provides the ability to perform the following measurement functions $(F1 \div F15)$: mapping and filtering of polarization images of BL; mapping of Stokes vector elements, azimuths, polarization ellipticals and phase shifts of polarization of biological structure; calculation of distributions of orientation, phase and orientation-phase MMI; reproduction of BL orientation and phase maps based on the corresponding MMI distributions and by direct methods; reproduction of orientation maps and phase maps of the outer and inner layers of a two-layer biological structure and the reproduction of MMI layers of a two-layer biological structure. The necessary measurements are realized by controlling the position of linear polarizers P1 and P2 capable to rotate the polarization plane of radiation to angles $0°; +45°; 90°; -45°; \theta°$, and phase quarter-wave plates PP1, PP2, PP3, the axes of which are rotated to angles $+45^{\circ}; +45^{\circ}; -45^{\circ}$, there is also the ability to eliminate elements from the path of laser radiation. As a result of realization of the analysis functions $(F16 \div F20)$, a set of informative indicators for each of the measured parameters of the structure of the investigated sections of BL is determined with the possibility of classification of "norm - severity of pathology" that is implemented by the expert system.

Results of experimental polarization reproduction of MMI of the layers of the smooth muscle of the cervix in the "normal" and "oncological" states submits the diagnosis possibilities of methods mentioned above realized by the system illustrated in figure 5.

In the research the two histological sections (geometric thickness 60 μm, optical thickness 0.1) of two-component cervix tissue “muscle tissue (MT) - connective tissue (CT)” were selected respectively in the “normal” and “oncology” states.

The researches were carried out on the experimental setup of the system shown in Fig. 4 by the method of Mueller-matrix reproduction and analysis of MMI “screened” outside (internal) partial layers of two-layer biological structures.

To detect changes in the structural anisotropy parameters, the orientation and phase Mueller-matrix image $\mathbf{B}_{22}(X,Y)$ and $\mathbf{B}_{44}(X,Y)$ of the relevant histological sections were selected.

Mueller-matrix images of the polarized reproducible orientation element $\mathbf{B}_{22}(X,Y)$ of the partial layer of healthy (left part) and oncologically altered (right part) smooth muscle tissue of a two-layer biological structure "muscle tissue (MT) - connective tissue (CT)" are shown in Fig. 5.

Fig. 6 illustrates autocorrelation functions and power spectra of coordinate distributions of an element $\mathbf{B}_{22}(X,Y)$ of both types of the cervix biological tissues.

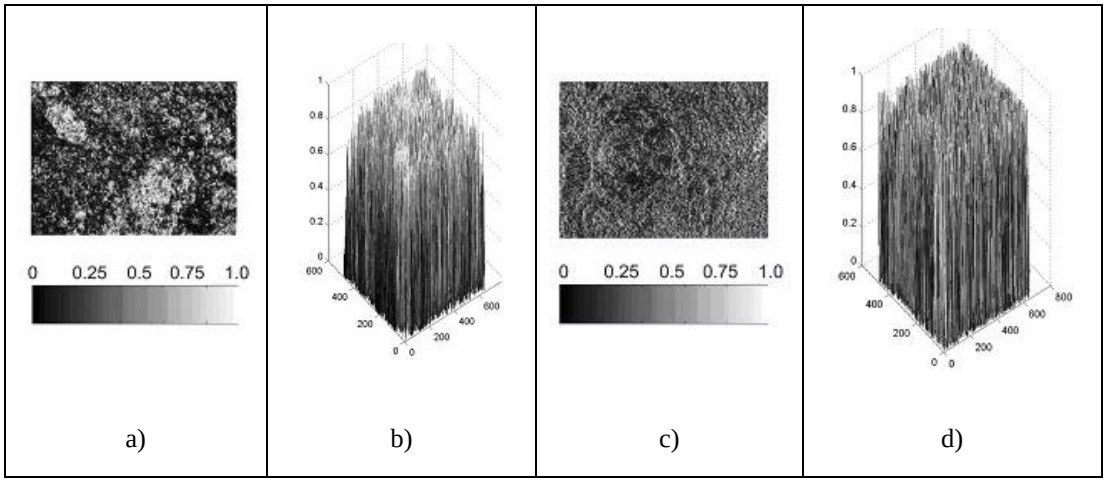

Figure 5. Polarized reproduced distribution of MMI of the smooth muscle of the cervix: a) 2D distribution at "norm"; b) 3D distribution at "norm"; c) 2D distribution at "pathology"; d) 3D distribution at " pathology ".

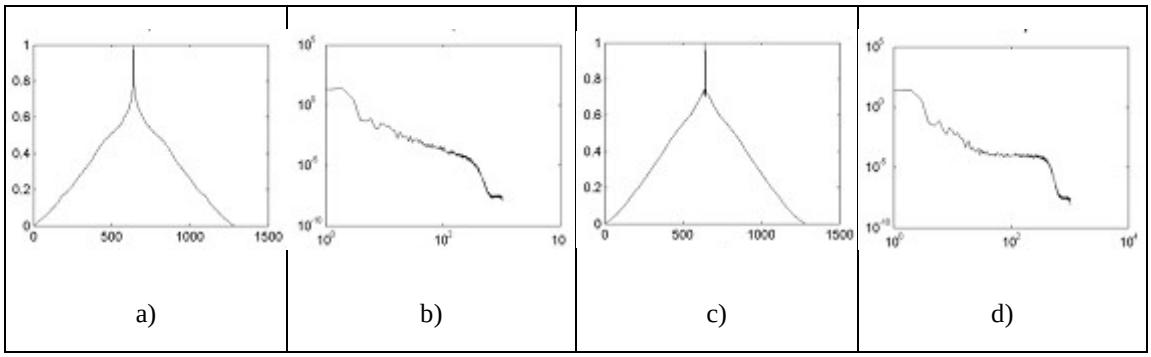

Figure 6. Characteristics of polarization-reproduced of the MMI of the smooth muscle of the cervix: a) ACF MMI at "norm"; b) power spectrum at " norm "; c) ACF MMI at " pathology "; d) power spectrum at "pathology".

Table 1 shows the values of the statistical characteristics of the coordinate, autocorrelation and spectrum distributions of experimentally measured $\mathbf{B}_{22}(X,Y)$ and $\mathbf{B}_{44}(X,Y)$ (optically thin layers of healthy smooth muscle tissue and in the state of dysplasia) and polarization reproduced (two-layer structure "smooth muscle - connective tissue") matrix elements $\mathbf{B}^{*}_{22}(X,Y)$ and $\mathbf{B}^{*}_{44}(X,Y)$. Analysis of the data in table 1 shows that the Mueller-matrix reproduction of the polarization properties of the optically anisotropic structure of the smooth muscle of the two-layer cervix of different physiological states allows to obtain the maximum differences between the experimental and reproduced due to polarization parameters, which do not exceed 35% - 40% while maintaining the general tendencies of their change.

Table 1 - Evaluation of the characteristics of the element distribution of experimentally measured and polarized MMI tissue of the cervix smooth muscle

State	Norm	Pathology	Norm	Pathology
	$\mathbf{B}^{*n}_{22}$	$\mathbf{B}^{*n}_{22}$	$\mathbf{B}^{*n}_{44}$	$\mathbf{B}^{*n}_{44}$
M_1	0,27*	0,33*	0,21*	0,25*
M_2	0,2*	0,11*	0,1*	0,11*
M_3	0,36*	3,77*	0,19*	0,56*
M_4	3,91*	6,71*	1,14*	4.99*
Q_2	0,24*	0,22*	0,23*	0,17*
Q_3	0,41*	0,93*	0,18*	0,24*
Q_4	1,42*	3,19*	0,74*	1,11*
W_1	0,57*	0,63*	0,68*	0,72*
W_2	0,19*	0,32*	0,12*	0,28*
W_3	0,12*	0,21*	0,15*	0,29*
W_4	0,32*	0,68*	0,22*	0,36*

In addition, the high sensitivity of the parameters $M_{i=1;2;3;4}$, $Q_{i=2;3;4}$ and $W_{i=1;2;3;4}$, which characterize the coordinate, correlation and self-similar structure of the orientation and phase MMI of all the considered groups of biological tissues for changing their physiological state, was realized.

The most informative parameters for differentiation of a healthy and oncologically modified layer of tissue of the cervix smooth muscle by their polarized MMI are the following:

1. Estimation of the central moments from the second to the fourth order $M_{2;3;4}$ coordinate distributions $\mathbf{B}_{22}^{*н}(X,Y)$ and $\mathbf{B}_{22}^{*п}(X,Y)$; $\mathbf{B}_{44}^{*н}(X,Y)$ and $\mathbf{B}_{44}^{*п}(X,Y)$, differences between which range from 2 (M_2) to 10 (M_3) times for "norm" and "pathology".

2. Estimation of the central moments from the second to the fourth order (Q_3), (Q_4) autocorrelation distributions $\mathbf{B}_{22}^{*н}(X,Y)$ and $\mathbf{B}_{22}^{*п}(X,Y)$; $\mathbf{B}_{44}^{*н}(X,Y)$ and $\mathbf{B}_{44}^{*п}(X,Y)$, differences between which range from 2 (Q_3) to 2,5 (Q_4) times for "norm" and "pathology".

3. Estimation of the central moments from the second to the fourth order (W_2), (W_3) power spectra $\mathbf{B}_{22}^{*н}(X,Y)$ and $\mathbf{B}_{22}^{*п}(X,Y)$; $\mathbf{B}_{44}^{*н}(X,Y)$ and $\mathbf{B}_{44}^{*п}(X,Y)$, differences between which range from 2 (W_2) to 3 (W_3) times for "norm" and "pathology".

5. EVALUATION OF THE RELIABILITY OF THE METHODS OF POLARIZATION-PHASE REPRODUCTION AND ANALYSIS

The effectiveness of the application of the suggested methods of polarization-phase reproduction and analysis of the polycrystalline structure of BL implemented by the experimental system was investigated on the example of differentiation of two rat liver samples: samples of "healthy" rats (group 1) and samples of rats "with hepatitis" (group 2). In each group, there were $N_1 = N_2 = 43$ two-layer optically thin frozen samples of rat liver BL, the diagnoses of which were previously verified using the histopathological examination method defined as the "gold standard". The previously accepted confidence probability level was p=0.95. For each method, the mean of $\bar{q}$ in the groups of values of statistical characteristics $M_{i=1\div4}, Q_{i=1\div4}, W_{i=1\div4}$ was determined, which describe the coordinate distributions, ACF and power spectra of the element distributions of the parameters measured, and their standard deviations $\pm\sigma$. On the basis of the most sensitive statistical characteristics $(\bar{q} \pm \sigma)$ of the distributions of the parameters measured, which provided statistical reliability of differences between groups (diagnostic informative features), differentiation of the states of "healthy" - "with hepatitis" samples of rat liver BL was performed.

In fig.7, fig. 8 two-dimensional phase distributions obtained by direct phase $\delta(X,Y)$ reproduction for histological sections of the rat liver in group 1 and group 2 are shown.

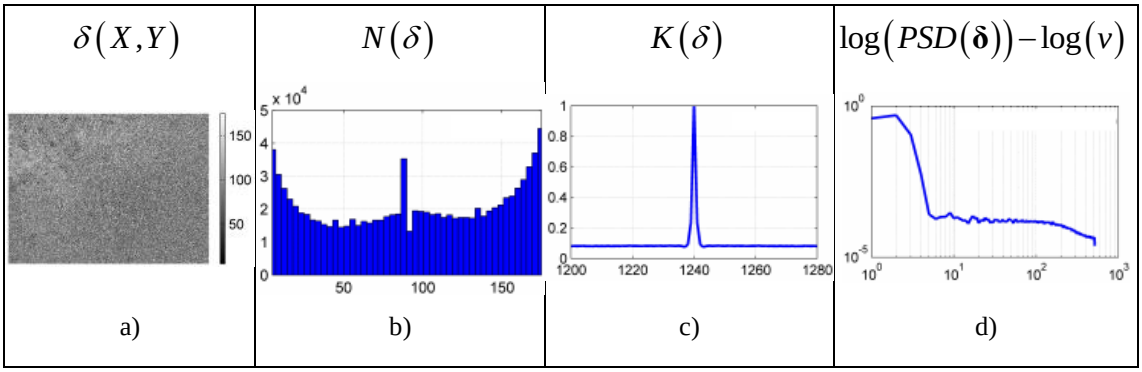

Figure 7 - Characteristics of a phase map reproduced by direct polarization reconstruction of the sample of rat liver BL of group 1: a) coordinate distribution; b) histogram; c) ACF distribution; d) the power distribution spectrum.

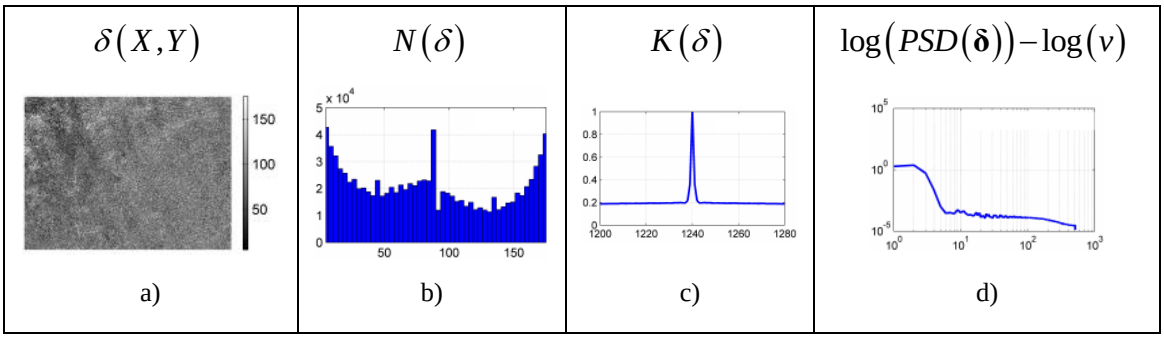

Figure 8 - Characteristics of a phase map reproduced by direct polarization reconstruction of the sample of rat liver BL of group 2: a) coordinate distribution; b) histogram; c) ACF distribution; d) the power distribution spectrum.

The mean $\overline{g}$ of the samples of group 1 and group 2 of the statistical characteristics $\left(M_{i=1;2;3;4}(\boldsymbol{\delta})\right)$ $\left(K_{i=1;2;3;4}(\boldsymbol{\delta})\right)$, $\left(W_{i=1;2;3;4}(\boldsymbol{\delta})\right)$ and their standard deviation for phase maps obtained on the basis of the experimental direct method are given in Table 2.

Table 2 - Statistical characteristics of coordinate distributions, ACFs and power spectra of phase distributions of rat liver BL obtained by a direct phase reproduction

g	**Group 1**	**Group 2**	g	**Group 1**	**Group 2**
M_1	0,19 ± 0,017	0,27 ± 0,023	W_1	0,61 ± 0,056	0,67 ± 0,059
M_2	0,23 ± 0,021	0,35 ± 0,029	W_2	0,21 ± 0,018	0,28 ± 0,023
M_3	0,51 ± 0,047	0,86 ± 0,077	W_3	0,15 ± 0,012	0,18 ± 0,015
M_4	0,45 ± 0,039	0,25 ± 0,022	W_4	0,19 ± 0,016	0,24 ± 0,021
Q_2	0,12 ± 0,011	0,15 ± 0,013			
Q_3	0,09 ± 0,009	0,11 ± 0,01			
Q_4	1,22 ± 0,11	0,79 ± 0,068			

Using the method of a direct polarization reproduction of the distribution of BL phase parameters, there is an upper limit of confidence in the differentiation of the histological sections structure of healthy and hepatic rat liver is 89.5%.

The reliability of differentiation of the structure of two-layer histological sections of the liver of healthy and hepatitis rats based on the three methods considered (Table 6) was increased in comparison with the known methods of Stokes polarimetry and analysis of multilayer BL [].There is Ac - accuracy (overall precision of differentiation of states norm pathology), Se - sensitivity of diagnosis, Sp - specificity of diagnosis in Table 3

Methods of a direct reproduction and analysis of distributions of orientation and phase parameters of polycrystalline BL networks allowed to increase the reliability of the assessment of pathological conditions of rat liver by 1% and 2.3% respectively, in comparison with the improved methods of reproducing the orientation and phase parameters of the BL structure based on its Mueller matrix mapping. The method of Mueller-matrix reproduction of the phase structure of "screened" outside BL provided maximum level of differentiation of accuracy of states “norm” – “pathology” of 95.3% that was increased by 5% compared to the reliability of the method of polarization mapping and analysis of phase Mueller-matrix images of BL.

Table 3 – Comparison of reliability of polarization-phase methods reproduction and analysis of BL structure

Methods name	**Quality level of evaluation**	*Ac*, %	*Se*, %	*Sp*, %
Method and system of direct polarization reproduction and analysis of the phase parameters distribution of an optically thin biological tissue	High	89,5	88,4	91
Method of a direct polarization reproduction and analysis of the orientation parameters distribution of an optically thin biological tissue	Good	83,7	83,7	83,7
Method and system of Mueller-matrix reproduction of coordinate distributions of orientation and phase parameters of the structure of "screened" outside layers of optically thin two-layer biological tissue	Excellent	95,3	95,3	95,3

CONCLUSIONS

A new group of methods and systems of reproduction and analysis of orientation and phase parameters of biological layers structure that can be used for evaluation of pathological states of histological sections was developed.

Methods of a direct reproduction and analysis of coordinate distributions of orientation and phase parameters of structure anisotropy of optical thin BL realize the instant formatting of polarimetric visualization conditions of phase anisotropy parameters of BL polycrystalline network and give the possibility to obtain the accuracy of the differentiation of "normal" - "hepatitis" states of rat liver of 83.7% and 89.5%.

Using the method of Mueller-matrix reproduction of coordinate distributions of orientation and phase parameters of the structure of "screened" outside layers of optically thin two-layer biological tissue for evaluation of the pathological states mentioned above increases the accuracy of diagnosis up to 95.3%.

REFERENCES

[1] Ghosh, N. and Vitkin, I. A., "Tissue polarimetry: concepts, challenges, applications, and outlook," Journal of Biomedical Optics 16(11), 110801 (2011).

[2] Tuchin, V. V., "Polarized light interaction with tissues," Journal of Biomedical Optics 21(7), 071114 (2016).

[3] Ushenko, Y. A., Boychuk, T. M., Bachynsky, V. T. and Mincer, O. P., [Handbook of Coherent-Domain Optical Methods], Springer Science+Business Media, New York, 107–148 (2013).

[4] Boer, J. F., Milner, T. E. and Nelson, J. S., "Determination of the depth-resolved Stokes parameters of light backscattered from turbid media by use of polarization-sensitive optical coherence tomography," Optics Letters 24, 300–302 (1999).

[5] Alalia, S. and Vitkin, A., "Polarized light imaging in biomedicine: emerging Mueller matrix methodologies for bulk tissue assessment," Journal of Biomedical Optics 20(6), 061104 (2015).

[6] Shukla, P., Pradhan, A., "Mueller decomposition images for cervical tissue: Potential for discriminating normal and dysplastic states," Optics Express 17(3), 1600–1609 (2009).

[7] Smith, M. H., Burke, P. D., Lompado, A. et al., "Mueller matrix imaging polarimetry in dermatology," Proc. of SPIE 3911, 1605-7422 (2000).

[8] Chung, J., Jung W., Hammer-Wilson, M. J., et al., "Use of polar decomposition for the diagnosis of oral precancer," Applied Optics 46(15), 3038–3045 (2007).

[9] Liu, G. L., Li, Y. and Cameron, B. D., "Polarization-based optical imaging and processing techniques with application to the cancer diagnostics," Proc. of SPIE 4617, 208–220 (2002).

[10] Pierangelo, A., Nazac, A., Validive, P. et al., "Polarimetric imaging of uterine cervix: a case study," Optics Express 21(12), 14120-14130 (2013).

[11] Ushenko, A. G. and Pishak, V. P., [Laser polarimetry of biological tissue. Principles and applications. Chapter in the book Biomedical Diagnostics, environmental and material Science], Kluwer Academic Publishers, Netherlands, 93–136 (2004).

[12] Dubolazov, A. V., Telenga, O. Yu. and Karachevtcev, A. O., "Polarization metrology of Mueller matrices images of biological tissues phase – inhomogeneus layers" Proc. of SPIE 7388, 73881F(2009).

[13] Zabolotna, N. I. and Musiichuk, I. V., “Principles and methods of Mueller-matrix tomography of multilayer biological tissues," Proc. SPIE 8338, 833810 (2011).
[14] Zabolotna, N. I., “Polarization laminated cartography of multilayer biological tissues," Proc. SPIE 8338, 833815 (2011).
[15] Zabolotna, N. I., Wojcik, W., Pavlov, S. V., Ushenko, O. G. and B. Suleimenov, "Diagnostics of pathologically changed birefringent networks by means of phase Mueller matrix tomography," Proc. SPIE 8698, 86980C (2013).
[16] Zabolotna, N. I., Dovhaliuk, R. Y., “Orientational tomography of optical axes directions distributions of multilayer biological tissues birefringent polycrystalline networks,” Proc. SPIE 8873, 887313 (2013).
[17] Zabolotna, N. I., Oliinychenko, B. P., Radchenko, K. O., Krasnoshchoka, A. K., Shcherba, O. K., “System of polarization phasometry of polycrystalline blood plasma networks in mammary gland pathology diagnostics,” Proc. of SPIE 9613, 961311 (2015).
[18] Zabolotna, N. I., Radchenko, K. O., Tarnovskiy, M. H., ” System of Mueller-Jones matrix polarizing mapping of blood plasma films in breast pathology,” Proc. SPIE 10407, 1040714 (2017).
[19] Zabolotna, N. I., Radchenko, K. O., “Multifunctional automated system of 2D laser polarimetry of biological tissues,” Proc. SPIE 9205, 92050V (2014).
[20] Ushenko, Y. A., Dubolazov, A. V., Karachevtcev, A. O., Zabolotna, N. I., “A fractal and statistic analysis of Mueller-matrix images of phase inhomogeneous layers,” Proc. SPIE 8134, 81340P (2011).
[21] Ushenko, A. G., Misevich, I. Z., Istratiy, V. et al., “Evolution of statistic moments of 2D-distributions of biological liquid crystal net Mueller matrix elements in the process of their birefringent structure changes,” Proc. SPIE 4231, 423145(2010).
[22] Angelsky, O. V., Ushenko, A. G., Ushenko, Y. A. et al., [Statistical, correlation, and topological approaches in diagnostics of the structure and physiological state of birefringent biological tissues], CRC Press, USA, 21–67 (2010).